S-310JA-1 ROCKET OBSERVATION OF VLF EMISSION SPECTRA AT SYOWA STATION IN ANTARCTICA

Iwane Kimura, Hisao Yamagishi, Toshiro Matsuo

Department of Electrical Engineering II, Kyoto University,
Sakyo-ku, Kyoto 606

and

Tetsuo Kamada

Research Institute of Atmospherics, Nagoya University,
Honohara, Toyokawa 442

Abstract: VLF chorus observed in geomagnetically quiet condition by an Antarctic rocket S-310JA-1 is discussed in detail in comparison with that observed on the ground (Syowa Station). The chorus intensity at the rocket altitudes was roughly $E = 18 \, \mu V/m$ and $H = 5 \times 10^{-12} T$ for a bandwidth of 50 Hz which proved the chorus propagation being in the whistler mode.

The upper cutoff frequency of the chorus spectra observed on the ground was always lower than that observed by the rocket. The difference of the upper cutoff frequency is interpreted by the frequency characteristics of both the effect of perfect reflection of the chorus at the bottom of the ionosphere and the collisional damping.

Static noise phenomena were also observed by the same rocket which will be reported in our future paper.

1. Introduction

Rocket observations of wave-particle interaction phenomena at Syowa Station (69.00°S, 39.58°E geographic; 66.7°S, 72.5°E geomagnetic; dip 65.4°) have been planned by using the S-210 type of rockets and a bigger type of rockets, the S-310 type which was newly developed by ISAS, University of Tokyo especially for the IMS Antarctic rocket program of the National Institute of Polar Research.

The purpose of these observations are mainly to observe energy spectra of soft electrons, and VLF and HF noise spectra, as well as electron density and temperature in the ionosphere, by which we investigate an association among these data. A relationship between the VLF noise in the ionosphere and those observed on the ground is also one of the interesting subjects of our experiment.

51

The first S-310 type rocket, S-310JA-1 was successfully launched from Syowa Station at 12:45 LT on February 13, 1976 by the members of the 17th Japanese Antarctic Research Expedition. The rocket reached an altitude of 215.6 km at 226 sec after launch, and its impact was 280 km toward a direction of 315° from the launching site. The geomagnetic activity at the time of rocket flight was very quiet.

As to the VLF observation, we could observe chorus by the instrument called PWL (Plasma Wave in VLF range) on board the rocket and by the ground receiver at the same time. By the rocket, another interesting wave phenomena were also observed, which did not look like electromagnetic wave phenomena. They might be electrostatic ones (GURNETT and MOSIER, 1969; MATSUMOTO et al., 1975).

No clear association of chorus intensity and energy spectra of keV electrons simultaneously observed by the rocket was found. The VLF static wave phenomena also observed by the rocket will be discussed in the future paper.

2. Rocket Borne Receiver

By PWL receiver on board the rocket VLF wave spectra in electric (E) and magnetic (H) fields in space were observed in the frequency range from 0.1 to 10 kHz, by an electric dipole antenna (2.8 m tip to tip) and by a loop antenna (8000 turns on a 10 mm $\phi \times 150$ mm long ferrite core). The antenna outputs were fed to each preamplifier (E and H). After having passed the preamplifiers, the E and H signals were alternatively fed to a common main amplifier by time sharing, 16 seconds for E channel and 8 seconds for H channel, as shown in the block diagram of Fig. 1. The outputs of the main amplifier were sent to the ground by means of a wide band (10 kHz) telemetry. This wide band telemeter-
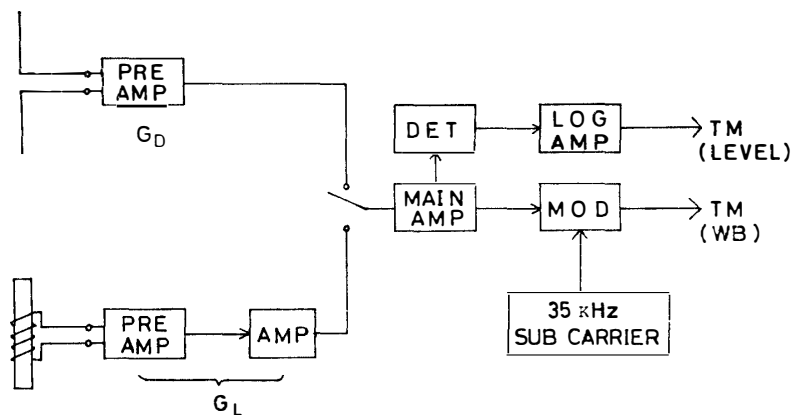

Fig. 1. Block diagram of the VLF instrument PWL.

ing was realized by VSB (Vestigial sideband amplitude modulation); the sub-carrier frequency being 35 kHz and a lower side band locating from the center (35 kHz) to 25 kHz.

During the above 16 seconds of time sharing for the E field, a 3 volt DC bias was applied to the dipole antenna for the first 8 seconds and no bias was applied for the second 8 seconds. The DC bias was aimed to remove the ion sheath which would be constructed around the dipole antenna when no DC bias
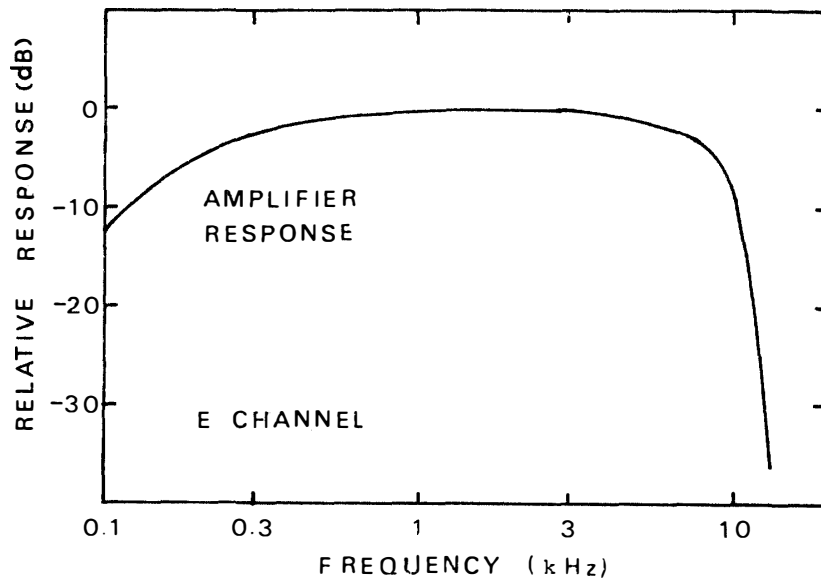

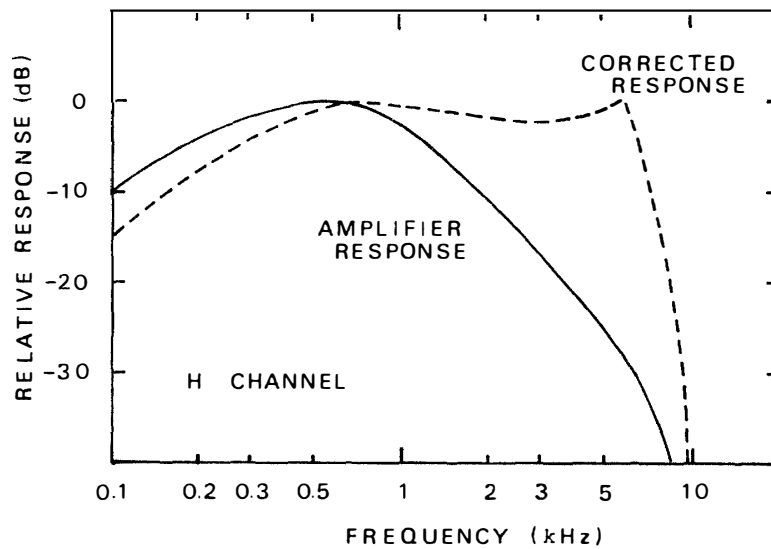Fig. 2. Frequency response of the overall E channel amplifier.

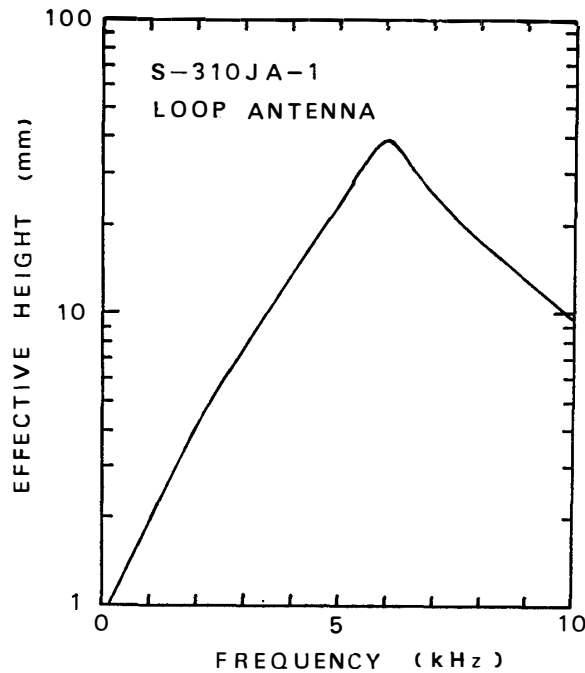Fig. 3. Frequency response of the overall H channel amplifier.

Fig. 4. Effective height of the loop antenna in free space.

was applied. The envelope level of the time shared wide band signals was sent to the ground by an IRIG telemetry channel.

The frequency dependence of the overall amplifier for the E channel is shown in Fig. 2. The pick up factor of the dipole antenna had also a frequency dependence, because the input resistance of the preamplifier was about 5 kΩ and the sheath capacitance was of the order of several tens pF. The threshold input level of the preamplifier was of the order of 1 μV.

The frequency dependence of the overall amplifier for the H channel is illustrated in Fig. 3. The effective height of the loop antenna in free space is shown in Fig. 4. The threshold input level of the preamplifier was of the order of 2 μV at 1 kHz. The overall dynamic range of the pre- and main amplifier was around 40 dB.

3. VLF Phenomena Observed by the Rocket

The envelope level of the wide band signals telemetered to the ground was recorded by a pen oscillograph, as shown in Fig. 5. An 8 second interval as assigned by "L" corresponds to the loop output signal (H channel), "D(3)" corresponds to the dipole output signal (E channel) when 3V DC was applied to the antenna, and "D(0)" corresponds to the dipole output signal when no DC voltage was applied. The intensity scale on the left indicates the input signal
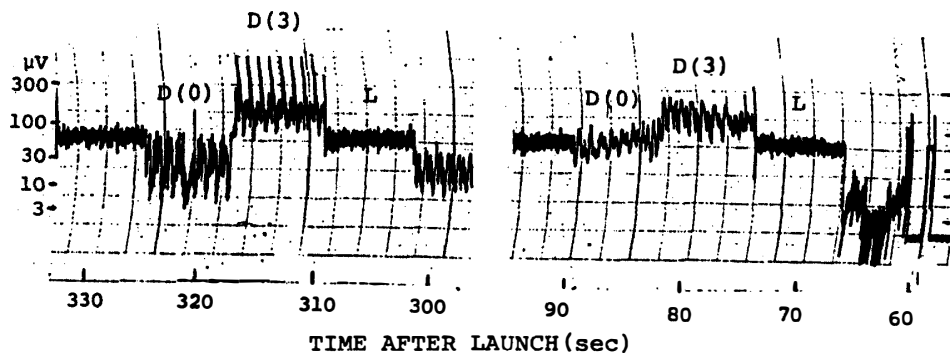
Fig. 5. An example of the amplitude envelope level of the wideband spectra recorded by a pen-oscillograph.
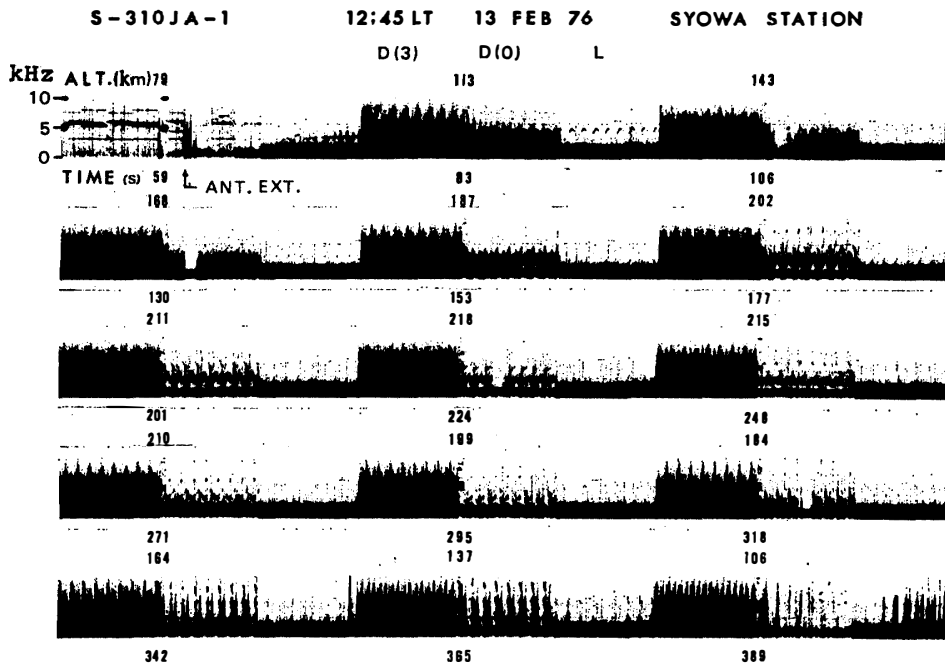

Fig. 6. An example of the frequency spectra of the VLF wideband signals.

strength at the dipole preamplifier inlet, so that it is only for E field. Spikes appearing in the record are rocket spin modulation.

Frequency spectra of the VLF wide band signals analyzed by a frequency analyzer is illustrated in Fig. 6.

A part of the spectra is also analyzed by a sonagraph. Fig. 7 is a sonagram of the case D(3) for an altitude of 212 km. In this sonagram, there are two types of VLF phenomena. The one is discrete emission whose intensity and frequency varies periodically twice within one rocket spin period (∼1 sec). The
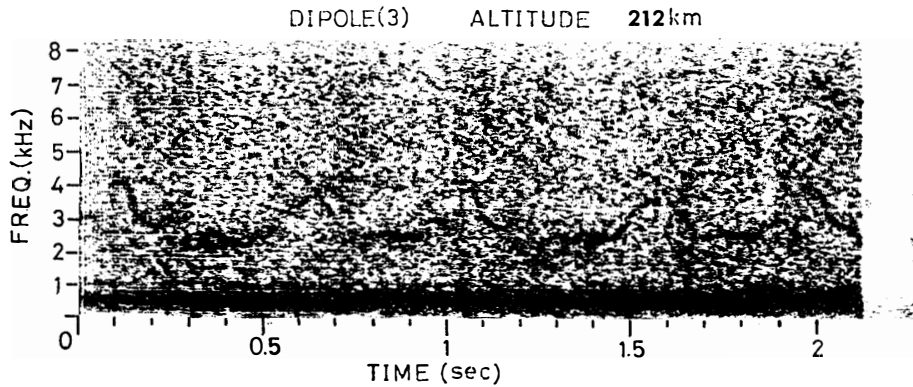
DIPOLE(3)   ALTITUDE   212km

Fig. 7.   Typical sonagram of VLF phenomena.

other is an emission whose frequency is limited below about 1 kHz and whose intensity is relatively independent of the rocket spin motion.

On the other hand, in the simultaneous ground observation, only a emission whose frequency is limited below 1 kHz, was observed as shown in Fig. 8. This is actually corresponding to that observed by the rocket in the same frequency band. Although this low frequency emission has no clear rising structure on the sonagram, it may be considered as chorus. This chorus was also observed by the loop antenna, channel "L", but it did not so clearly appear on the wide band
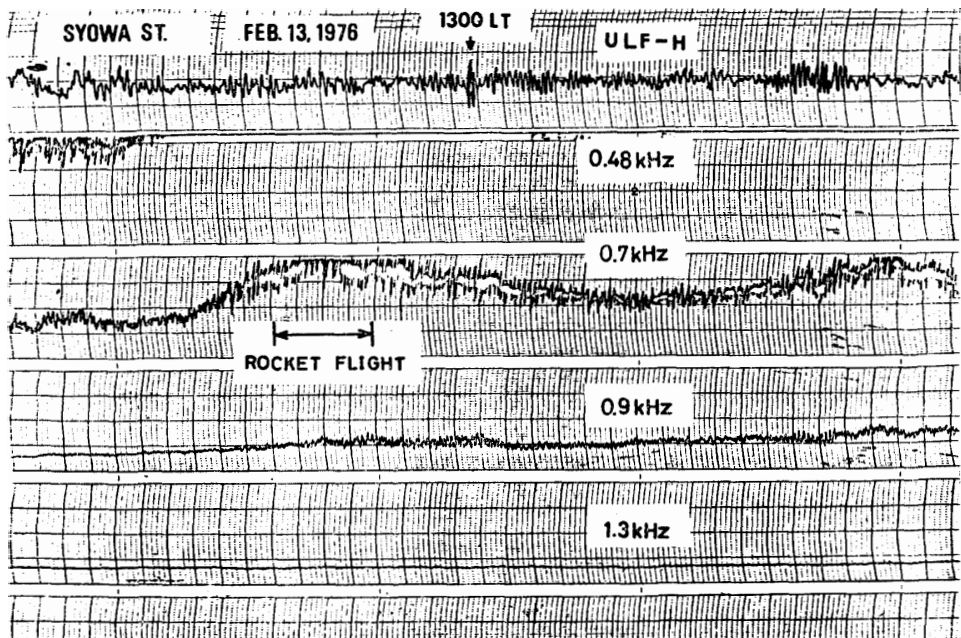

Fig. 8.   Fixed frequency amplitude variations of VLF emissions at 0.48, 0.7, 0.9 and 1.3 kHz and H component of ULF emissions observed at Syowa Station around the time of the rocket launching.

spectra due to an interference by a rocket borne radar transponder. In the present paper, the characteristics of this chorus are discussed.

The discrete emissions observed by the rocket, but not observed by L channel of the rocket and on the ground can be considered as a static wave phenomenon, which will be reported in detail in our future paper.

4. Altitude Variation of the Electric Field of Chorus

The chorus component was extracted by a low pass filter of 1.25 kHz from the wide band signal. Detected envelope of the LPF output was recorded by a penoscillograph. In Fig. 9, the time variation of the envelope is shown. The
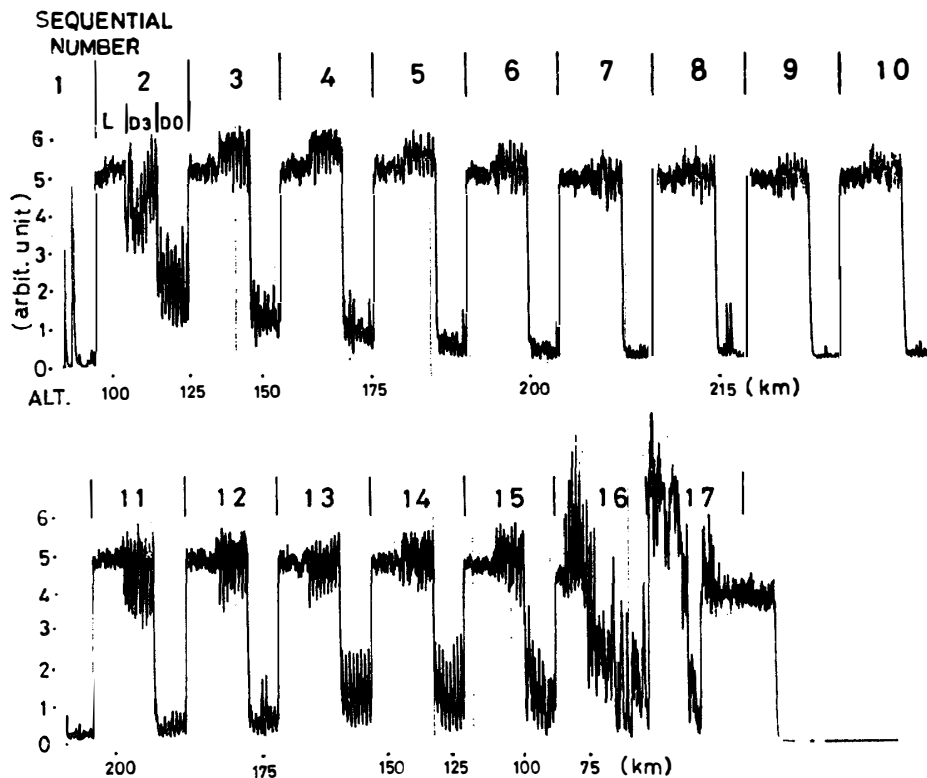

Fig. 9. Time variation of the detected envelope of the LPF (cutoff frequency 1.2 kHz) output of chorus component.

numbers above the pen record is sequential numbers, each corresponding to 24 seconds interval which consists of L (8 sec), D(3) (8 sec) and D(0) (8 sec) respectively as mentioned in the previous section.

From the figure, it can be seen that
1) the level L is almost unchanged with altitude,
2) the level D(3) first rises at altitudes around 110 km, peaks around the

altitude range from 130 to 160 km, then remains almost constant until the rocket descends down below 100 km,

3)   the level D(0) decreases monotonically with altitude both for ascending and descending legs.

The constant level of L is attributed to the interference from the radar transponder on board the rocket. The level change of D(3) is within 2 dB for altitudes above 100 km. On the other hand, the variation of D(0) is tremendous, the level decreasing about 20 dB from an altitude of 100 km to the apex. If the signal received is chorus and if its source level is almost constant with time, the electric field should remain almost constant in the altitude range from 110 to the apex of the rocket, because the electron density observed by the same rocket
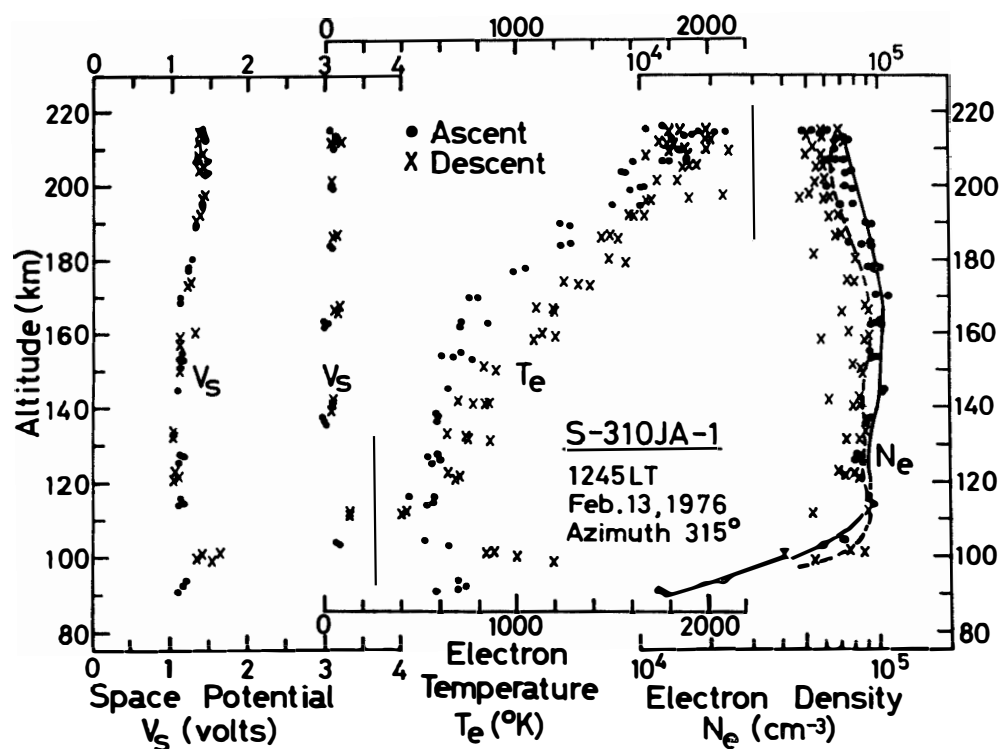

Fig. 10.   Electron density and temperature profile observed by the same rocket (after OGAWA et al., 1978).

was almost constant for the same range of altitude as shown in Fig. 10 (OGAWA et al., 1978). The tendency that the D(3) level is almost constant implies that the DC bias could remove the ion sheath around the antenna so perfectly that the received level actually indicated the real electric field of the chorus.

In the case of D(0), the ion sheath might affect the input level to the pre-amplifier due to an altitude variation of the sheath impedance.   Actually the

electron temperature T_e measured by Langmuir probe (OGAWA *et al.*, 1978) increased linearly with altitude from about 500 K at 100 km to 2000 K at apex as shown in Fig. 10. This altitude variation of T_e is, however, not sufficient to explain 20 dB change of D(0) level, if the sheath impedance is simply assumed to be proportional to $\sqrt{T_e/N_e}$ (AGGSON and KAPETANAKOS, 1966). This problem can not be fully resolved.

Absolute intensity of chorus could be determined from the intensity of the wide band spectra in reference to the 7 kHz calibration inserted every 24 seconds and the amplifier gain characteristics.

The estimated electric field of chorus at 500 Hz at an altitude of 142 km was about 18 μV/m. This field intensity was deduced from D(3) data, because the ion sheath effect could be ignored by the 3 volt bias.

The magnetic field of chorus determined from the wide band spectra of H channel was about 4 μAT/m (or 5×10^{-12}T $(10^{-9}$T$=1\gamma)$). The refractive index calculated from the ratio of E/H is about 84, which is very close to 101 that is calculated as the whistler mode from Appleton Hartree's equation under the plasma parameters, $f_0 = 2.85$ MHz and $f_H = 1.57$ MHz. These intensities seemed to be roughly independent of altitude.

5. Frequency Spectra of Chorus Simultaneously Observed by the Rocket and on the Ground

In Fig. 11, detailed sonagrams of the chorus are shown. The right side corresponds to the chorus observed by the rocket at altitudes around 134–144 km and 207–210 km and the left side corresponds to those simultaneously observed on the ground.

The above comparison of the spectra indicates that the upper cutoff frequency of the chorus observed on the ground is always lower than that observed by the rocket. On the other hand, the lower cutoff frequency at the rocket looks a little bit higher than that on the ground. However this tendency may be caused by the frequency response of the rocket borne amplifier shown in Fig. 2, so that the lower cutoff frequency at the rocket could be almost the same as that on the ground. The cutoff frequency is, therefore, around 200 Hz.

The above mentioned difference in the upper cutoff frequency should be due to lower ionospheric effects, if the chorus is originated in a very high altitude region. One effect is total reflection of the chorus at the bottom of the ionosphere, and the other is an absorption due to electron-neutral particle collisions in the lower ionosphere. These two effects will be discussed in the next section.
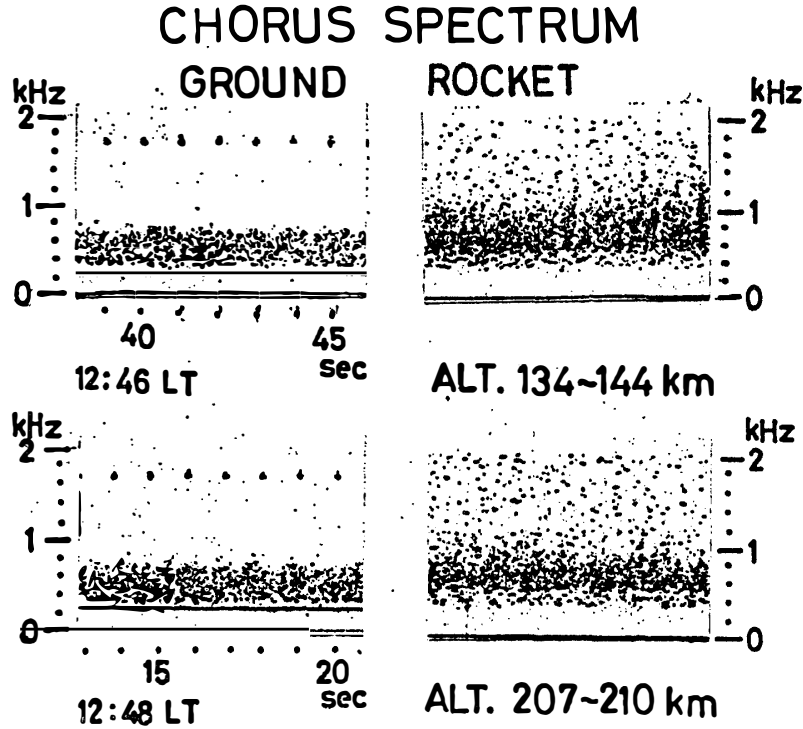
CHORUS SPECTRUM

Fig. 11.   Detailed sonagrams of the chorus.

6. Total Reflection and Collisional Absorption in the Ionosphere

Assume that a whistler mode wave starts to propagate downwards from a certain level in the higher ionosphere. The refractive index at the starting level is defined as $n_{init.}$ and the incident angle θ_i at the starting level is measured in reference to the vertically downward direction, when the ionosphere is assumed to be horizontally (planely) stratified. Then, the penetrating angle θ_0 in the free space below the ionosphere is given by Snell's law as follows.

$$N_{init.} \sin\theta_i = \sin\theta_0 \tag{1}$$

If $n_{init.}\sin\theta_i$ exceeds unity, there is no real θ_0, that is no penetrating component. In such a case the incident wave is thought to be perfectly reflected upwards at a level where the refractive index $n=n_{init.}\sin\theta_i$.

Wave-theoretically, however, this wave can reach the ground passing through the perfect reflection level, in an evanescent mode with the following amount of damping

$$\Gamma = 8.686 \, k_0 q_i h \text{ [dB]} \tag{2}$$

$$q_i = \text{Im}\sqrt{1 - n_{init.}\sin^2\theta_i}, \tag{3}$$

where h is the altitude of the perfect reflection level and $k_0(\equiv 2\pi f/c)$ is the wave number in free space. Im indicates an imaginary part of the quantity.

The above damping quantity Γ is unexpectedly small for low frequencies around several hundred Hz, and increases with increasing frequency.

In estimating θ_0, we take account of an effect of field aligned ionization ducts in the magnetosphere. If the chorus propagates from the source along the duct, the angle $\Delta\psi$ between the wave normal direction and the duct axis, has to satisfy the following condition (HELLIWELL, 1965),

$$\Delta\psi \lesssim \cos^{-1} N_b/N_m \qquad (4)$$

where N_b is the electron density in the background, and N_m is the maximum electron density at the center of the duct. For example, a 1.5% enhancement duct ($N_m/N_b = 1.015$) gives rise to a range of $\Delta\psi \leq 10°$, a 3.5% duct yields $\Delta\psi \leq 15°$ and a 5.1% duct yields $\Delta\psi \leq 18°$.

At Syowa Station, the geomagnetic dip angle is 65.4°, so that if the exit of the duct is assumed to be the starting level, the incident angle θ_i should be in the following range

$$24.6° - \Delta\psi \leq \theta_i \leq 24.6° + \Delta\psi. \qquad (5)$$

The refractive index at this level, $n_{\text{init.}}$ is given by

$$n_{\text{init.}} \cong \sqrt{f_p^2/f f_H \cos \theta}, \qquad (6)$$

where f is the frequency of the wave, f_p and f_H are the plasma and cyclotron frequency of electrons, and θ is the angle between the wave normal and the geomagnetic field line, which is identical with $\Delta\psi$ in eq. (4). Regorously, the effect of the coexisting ions must be taken into account for very low frequencies. However, it may be negligible, because we consider the right handed polarized whistler mode that propagates down to free space.

The limiting incident angle or transmission cone angle, θ_1, by which the wave can penetrate the ionosphere to the free space at Syowa Station is, according to eq. (1), given by

$$\sin \theta_i = \sqrt{f f_H \cos (24.6° - \theta_i)/f_p^2} \qquad (7)$$

where θ_0 is taken as 90° and in the range of θ_i determined by eq. (5) the minimum value is adopted for the optimum condition of penetration.

Let us assume that the altitude of the duct exit is 2000 km and that the plasma parameters are

$$f_p = 285 \text{ kHz}, \qquad f_H = 725 \text{ kHz}.$$

θ_i satisfying eq. (7) is, then, 1.8° for $f=100$ Hz, 5.4° for $f=1$ kHz and 17.4° for $f=10$ kHz.

Hereafter we also assume that the ionosphere below the altitude of the duct exit is planely (horizontally) stratified. Then, if the wave normal direction at the duct exit is within the above transmission cone, the wave can reach the ground without perfect reflection and without any attenuation, as far as the collisional damping is not taken into account. If the wave normal direction at the duct exit is outside the transmission cone, the wave is perfectly reflected at a certain level above the bottom of the ionosphere and then reaches the ground in an evanescent mode with the attenuation given by eq. (2). Now, for a particular θ_i which is determined by 24.6°-$\Delta\psi$, Γ is estimated as a function of frequency where h in eq. (2) is assumed to be 70 km and Γ is shown in Fig. 12 with $\Delta\psi$ as a parameter. From the figure, we find that the frequency dependence of the attenuation is strongly dependent on $\Delta\psi$ or the enhancement factor of the duct and that Γ increases with increasing frequency below a certain frequency
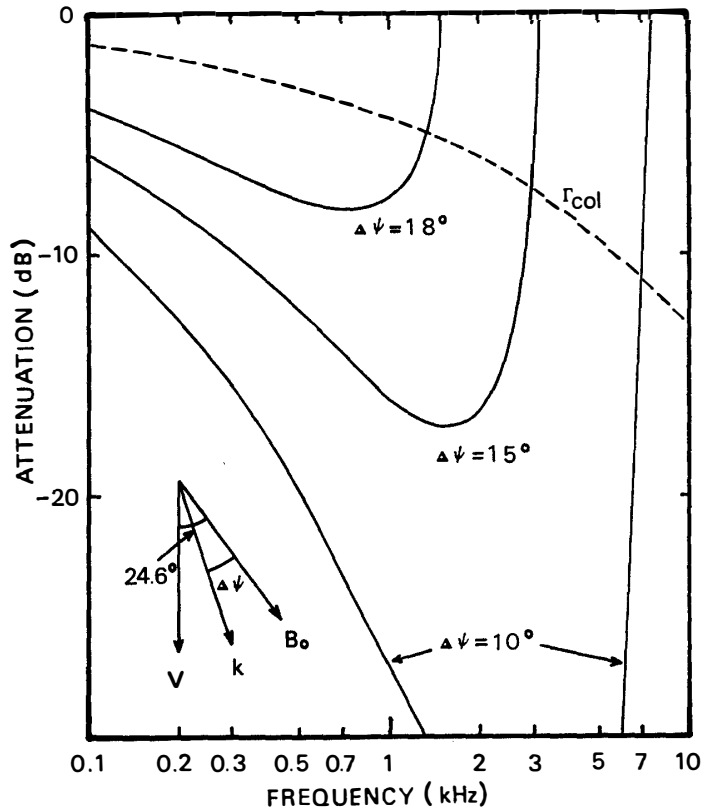

Fig. 12. Frequency dependence of the attenuation Γ after perfect reflection. The direction of geomagnetic field is 24.6° from the vertical (V).
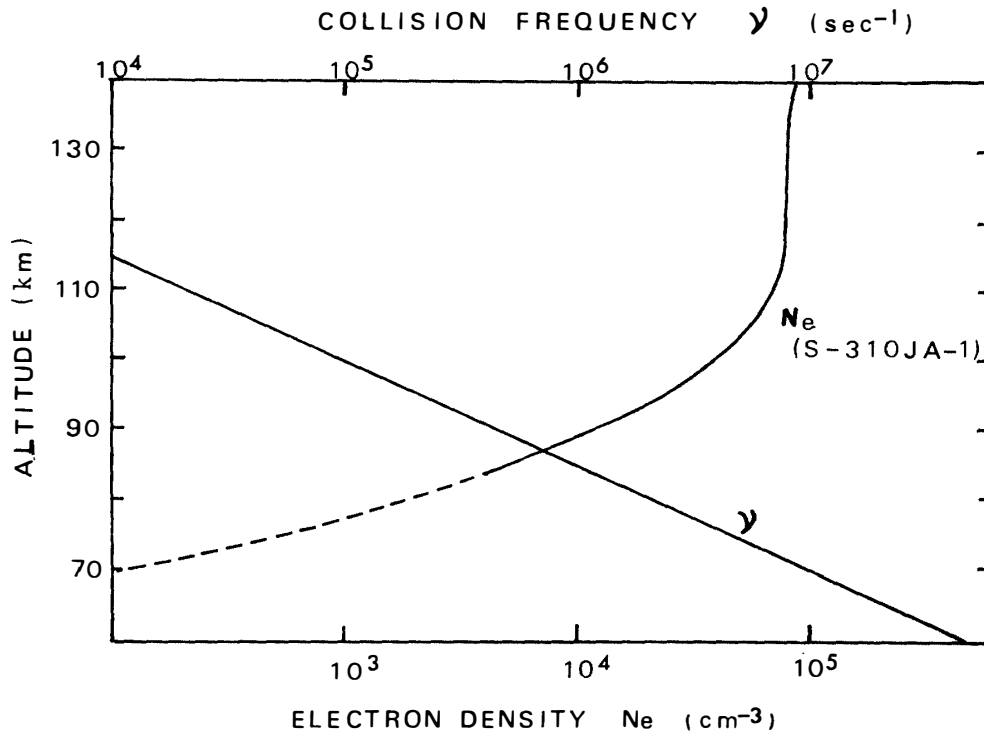
Fig. 13. *Electron density and collision frequency profiles used for the calculation of collisional damping.*

limit and the attenuation becomes zero above the limit, because the transmission cone is enlarged to contain the wave normal direction within the cone.

In the next step, we have to consider the effect of collisional damping. We now assume the collision frequency as shown in Fig. 13 and use the electron density profile observed by the same rocket S-310JA-1 (OGAWA *et al.*, 1978), which was extraporated from 85 km down to 70 km, as shown in Fig. 13. This density profile is very similar to the profile 'quiet ionosphere near noon in auroral zone' (ONDOH, 1963) that was used for the ionospheric absorption of VLF emission. The collisional damping for an altitude range from 100 to 70 km is calculated using these profiles. The dashed line in Fig. 12 is the frequency dependence of the damping. Then the total attenuation Γ_{total} is the sum of solid line and dashed line in Fig. 12. This characteristic can be the cause of the difference in frequency spectra which were observed at the rocket and on the ground.

For example, Fig. 14(a) illustrates spectral intensity of chorus observed by the rocket (at an altitude of 161 km) and on the ground, where the absolute intensity on the ground could not be determined because of the lack of absolute calibration. In Fig. 14(b), the solid line indicates the relative difference in the
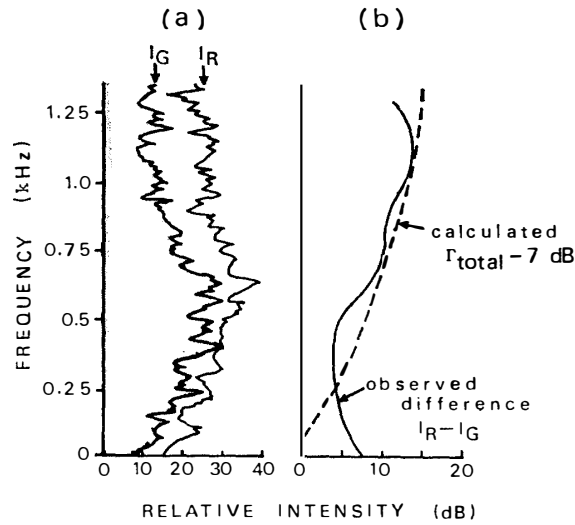
Fig. 14. *Relative difference in the spectral intensity observed by the rocket* (I_R) *and on the ground* (I_G). Γ_{total} *in* (b) *is the calculated sum of attenuation for the case* $\Delta\psi=15°$ *shown in Fig. 12.*

smoothed spectral intensity (in dB) by the both observations. On the other hand, the dashed line shows the frequency dependence of $\Gamma_{\text{total}}-7$dB calculated for the case $\Delta\psi=15°$ shown in Fig. 12. This case corresponds to a duct enhancement factor of 3.5%. It appears that the frequency dependence of the attenuation caused within the lower part of the ionosphere can be roughly explained by our proposed mechanism, if the duct enhancement factor was such a value as 3.5%.

Quantitatively, however, we have to know the absolute intensity of chorus on the ground. Moreover, in calculating the solid lines in Fig. 12, the ionosphere was assumed to be planely stratified for the altitude range from the bottom up to 2000 km. For more quantitative discussion, the spherical structure must be taken into account for the ionosphere.

7. Lower Cutoff Characteristics of the Chorus

The lower cutoff frequency of the chorus observed in our experiment was about 200 Hz both at the rocket and on the ground. This is partly due to the frequency characteristics of the receiver. There is, however, another cause which is due to the propagation characteristics of the chorus in the space from the source to the rocket altitudes.

In the ionosphere and magnetosphere the propagation characteristics at low frequencies are affected by existence of ions. Fig. 15 is an example of ion and electron density profiles above an altitude of 300 km. Due to the effect of multi-ions, there are several characteristic frequencies;
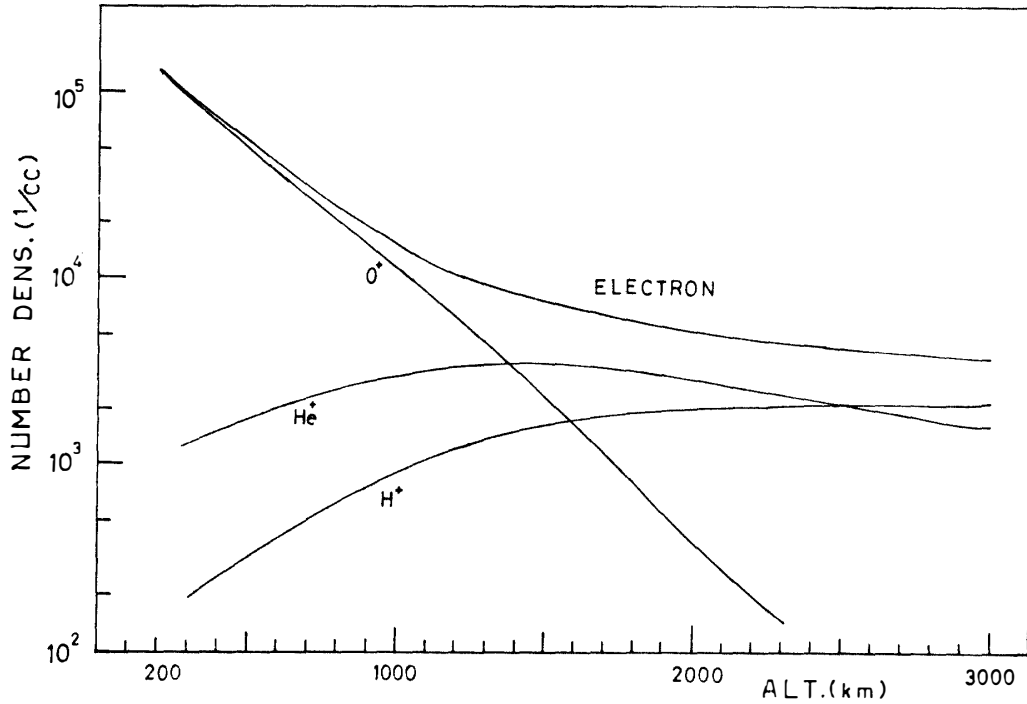
Fig. 15. Electron and ion density profiles above an altitude of 300 km.

1) Ion cyclotron (gyro) resonance frequency at $L=\infty$,

2) Crossover frequency at $R=L$,

3) Cutoff frequency at $L=0$,

where

$$R=1-\sum_{k}\frac{\pi_k^2}{\omega^2}\left(\frac{\omega}{\omega+\varepsilon_k\Omega_k}\right),$$

$$L=1-\sum_{k}\frac{\pi_k^2}{\omega^2}\left(\frac{\omega}{\omega-\varepsilon_k\Omega_k}\right),$$

π_k and Ω_k are plasma angular frequency and cyclotron angular frequency of the k-th species of the constituents, and the sign of the charge, ±1, is given by ε_k (STIX, 1962).

As shown in Fig. 16, at any altitude, there are two pairs of such characteristic frequencies by the effects of three species of ions whose densities are shown in Fig. 15. For example, consider a wave with a frequency 400 Hz starting at 3000 km. When it propagates down in the right handed polarized mode to an altitude of 1600 km, corresponding to the level $L=R$, the sense of polarization is reversed to become a left handed mode. It then propagates down to an altitude of 1500 km, where the left handed mode is perfectly reflected back at $L=0$
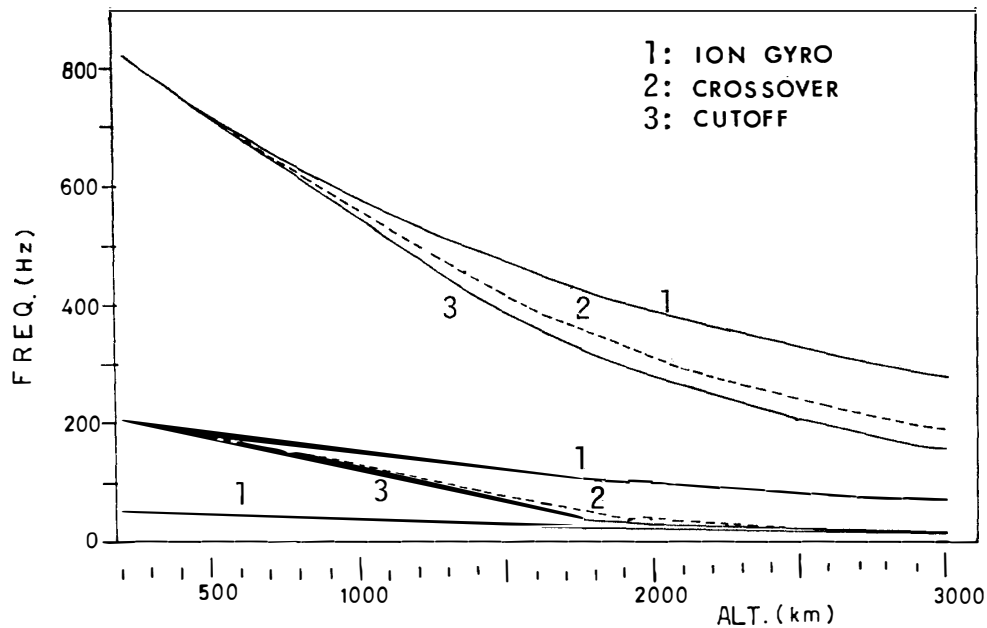
Fig. 16. Altitude profiles of the ion cycrotron (gyro), crossover and cutoff frequencies.

so that this mode can not reach the rocket and the ground. Actually, however, at the crossover frequency, the right handed polarized mode is mostly converted to the left handed polarized mode, but is partly to the right handed polarized mode by mode coupling. The latter mode can propagate to the ground without reflection at the level $L=0$. Therefore the wave with a frequency 400 Hz can be observed by the rocket and also on the ground with some attenuation due to the mode coupling at the level $L=R$.

For frequencies less than 200 Hz, the wave can also reach the rocket and the ground after two times of mode coupling as will be seen in Fig. 15. It can be therefore concluded that the waves of the frequencies below 200 Hz are more strongly attenuated than those above 200 Hz, although the mode coupling loss can not be quantitatively given here. This effect must be common for the low frequency spectra of chorus observed at altitudes below 200 km. The lower cutoff frequency of chorus observed by our rocket and on the ground, around 200 Hz incidentally coincides the frequency corresponding to the border line between one and two times the mode coupling that are required.

8. Conclusion

Geomagnetic activity on the ground when the S-310JA-1 was launched, was rather quiet. Cosmic noise absorption was about 0.8–1.0 dB. VLF chorus activity was high. In our rocket experiment, therefore, VLF chorus was observed. Particle

flux of electrons with energy from 1 to 10 keV was also observed by the experiment, but there was no clear association with the intensity or spectra of chorus. As another type of VLF wave phenomena, spin modulated discrete emissions were observed by the rocket, which was interpreted as an electrostatic phenomenon. The chorus intensity at the rocket altitudes was almost constant, being 18 μV/m in E field and 5×10^{-12} T in H for a bandwidth of 50 Hz which proved the chorus to be propagated in the whistler mode.

A difference in frequency spectra was found between the chorus observed by rocket and that observed on the ground. The difference in the upper cutoff frequency of spectra was interpreted by the frequency dependence of the transmission cone angle and the dependence of the attenuation in the evanescent mode suffering after perfect reflection, when the wave normal direction is outside the transmission cone.

Acknowledgment

References

AGGSON, T. L. and KAPETANAKOS, C. A. (1966): On the impedance of a satellite borne VLF electric field antenna. NASA-Goddard Space Flight Center, Greenbelt, Maryland, X-612-66-380, 42 p.

GURNETT, D. A. and MOSIER, S. R. (1969): VLF electric and magnetic fields observed in the auroral zone with the Javelin 8.46 sounding rocket. J. Geophys. Res., 74, 3979–3991.

HELLIWELL, R. A. (1965): Whistlers and Related Ionospheric Phenomena. Stanford Univ. Press.

MATSUMOTO, H., MIYATAKE, S. and KIMURA, I. (1975): Rocket experiment on spontaneously and artificially stimulated VLF plasma waves in the ionosphere. J. Geophys. Res., 80, 2829–2834.

OGAWA, T., MORI, H. and MIYAZAKI, S. (1978): Rocket measurements of daytime electron density and temperature profiles in the polar ionosphere. Mem. Natl Inst. Polar Res., Spec. Issue, 9, 1–11.

ONDOH, T. (1963): The ionospheric absorption of the VLF emissions at the auroral zone. J. Geomagn. Geoelectr., **15**, 90–108.

STIX, H. (1962): The Theory of Plasma Waves. New York, McGraw-Hill.